Bayesian chronological analyses consistent with synchronous age of 12,835–12,735 Cal B.P. for Younger Dryas boundary on four continents

James P. Kennett[a,1], Douglas J. Kennett[b], Brendan J. Culleton[b], J. Emili Aura Tortosa[c], James L. Bischoff[d], Ted E. Bunch[e], I. Randolph Daniel Jr.[f], Jon M. Erlandson[g], David Ferraro[h], Richard B. Firestone[i], Albert C. Goodyear[j], Isabel Israde-Alcántara[k], John R. Johnson[l], Jesús F. Jordá Pardo[m], David R. Kimbel[n], Malcolm A. LeCompte[o], Neal H. Lopinot[p], William C. Mahaney[q], Andrew M. T. Moore[r], Christopher R. Moore[j], Jack H. Ray[p], Thomas W. Stafford Jr.[s,t], Kenneth Barnett Tankersley[u], James H. Wittke[e], Wendy S. Wolbach[v], and Allen West[w,2]

[a]Department of Earth Science and Marine Science Institute, University of California, Santa Barbara, CA 93106; [b]Department of Anthropology, Pennsylvania State University, University Park, PA 16802; [c]Departament Prehistoria i Arqueologia, Universitat de Valencia, E-46010 Valencia, Spain; [d]Berkeley Geochronology Laboratory, Berkeley, CA 94709; [e]Geology Program, School of Earth Science and Environmental Sustainability, Northern Arizona University, Flagstaff, AZ 86011; [f]Department of Anthropology, East Carolina University, Greenville, NC 27858; [g]Museum of Natural and Cultural History, University of Oregon, Eugene, OR 97403; [h]Viejo California Associates, Joshua Tree, CA 92252; [i]Lawrence Berkeley National Laboratory, Berkeley, CA 94720; [j]South Carolina Institute of Archaeology and Anthropology, University of South Carolina, Columbia, SC 29208; [k]Instituto de Investigaciones Metalúrgicas, Departamento de Geología y Mineralogía, Universidad Michoacana de San Nicólas de Hidalgo, 58060 Morelia, Michoacán, Mexico; [l]Santa Barbara Museum of Natural History, Santa Barbara, CA 93105; [m]Departamento de Prehistoria y Arqueología, Facultad de Geografía e Historia, Universidad Nacional de Educación a Distancia, E-28040 Madrid, Spain; [n]Kimstar Research, Fayetteville, NC 28312; [o]Center of Excellence in Remote Sensing Education and Research, Elizabeth City State University, Elizabeth City, NC 27909; [p]Center for Archaeological Research, Missouri State University, Springfield, MO 65897; [q]Quaternary Surveys, Thornhill, ON, Canada L4J 1J4; [r]College of Liberal Arts, Rochester Institute of Technology, Rochester, NY 14623; [s]AMS ^{14}C Dating Centre, Department of Physics & Astronomy, University of Aarhus, 8000 Aarhus C, Denmark; [t]Centre for GeoGenetics, Natural History Museum of Denmark, Geological Museum, DK-1350 Copenhagen, Denmark; [u]Departments of Anthropology and Geology, University of Cincinnati, Cincinnati, OH 45221; [v]Department of Chemistry, DePaul University, Chicago, IL 60614; and [w]GeoScience Consulting, Dewey, AZ 86327

Edited by Mark H. Thiemens, University of California, San Diego, La Jolla, CA, and approved June 26, 2015 (received for review April 14, 2015)

The Younger Dryas impact hypothesis posits that a cosmic impact across much of the Northern Hemisphere deposited the Younger Dryas boundary (YDB) layer, containing peak abundances in a variable assemblage of proxies, including magnetic and glassy impact-related spherules, high-temperature minerals and melt glass, nanodiamonds, carbon spherules, aciniform carbon, platinum, and osmium. Bayesian chronological modeling was applied to 354 dates from 23 stratigraphic sections in 12 countries on four continents to establish a modeled YDB age range for this event of 12,835–12,735 Cal B.P. at 95% probability. This range overlaps that of a peak in extraterrestrial platinum in the Greenland Ice Sheet and of the earliest age of the Younger Dryas climate episode in six proxy records, suggesting a causal connection between the YDB impact event and the Younger Dryas. Two statistical tests indicate that both modeled and unmodeled ages in the 30 records are consistent with synchronous deposition of the YDB layer within the limits of dating uncertainty (~100 y). The widespread distribution of the YDB layer suggests that it may serve as a datum layer.

Younger Dryas | comet | Bayesian | radiocarbon | synchroneity

According to the Younger Dryas Impact Hypothesis (YDIH) (1), a major cosmic episode of multiple airbursts/impacts occurred at 12,800 ± 300 calendar years before 1950 (Cal B.P. represents calendar years before A.D. 1950, unless otherwise noted; 95% probability) or 12,950–12,650 Cal B.P. at 68% probability. This event produced the Younger Dryas boundary (YDB) layer, displaying peaks in a variable assemblage of spherules (glassy and/or magnetic—inferred to be impact ejecta and therefore, for simplicity, referred to below as impact-related spherules), high-temperature minerals and melt glass, nanodiamonds, charcoal, carbon spherules, glass-like carbon, aciniform carbon (soot), nickel, iridium, platinum, and osmium. The event may have triggered the Younger Dryas episode of abrupt climate change, contributed to the end-Pleistocene megafaunal extinctions, and initiated human population reorganization/decline across the Northern Hemisphere (1–5). Because a temporally singular event is proposed, the YDIH requires dates on the YDB layer to be essentially isochronous across four continents within the limits of dating methods.

In a test of synchroneity, it is ideal to have numerous, highly accurate, and precise dates to develop robust chronological models (6). The term "date" represents a measured value, and "age" refers to real or modeled calendar years. However, when developing high-precision chronologies, there are multiple challenges that are amplified in Pleistocene age deposits. Modern accelerator mass spectrometry (AMS) radiocarbon (^{14}C) measurements are typically very precise, with uncertainties of ±20 y to ±30 y at 11,000 ^{14}C years B.P., but high precision does not mean high accuracy. Numerous problems can produce erroneous ages

Significance

A cosmic impact event at ~12,800 Cal B.P. formed the Younger Dryas boundary (YDB) layer, containing peak abundances in multiple, high-temperature, impact-related proxies, including spherules, melt glass, and nanodiamonds. Bayesian statistical analyses of 354 dates from 23 sedimentary sequences over four continents established a modeled YDB age range of 12,835 Cal B.P. to 12,735 Cal B.P., supporting synchroneity of the YDB layer at high probability (95%). This range overlaps that of a platinum peak recorded in the Greenland Ice Sheet and of the onset of the Younger Dryas climate episode in six key records, suggesting a causal connection between the impact event and the Younger Dryas. Due to its rarity and distinctive characteristics, the YDB layer is proposed as a widespread correlation datum.

Author contributions: J.P.K., D.J.K., B.J.C., T.E.B., W.S.W., and A.W. designed research; J.P.K., D.J.K., B.J.C., J.E.A.T., J.L.B., T.E.B., I.R.D., J.M.E., D.F., A.C.G., I.I.-A., J.R.J., J.F.J.P., D.R.K., M.A.L., N.H.L., W.C.M., A.M.T.M., C.R.M., J.H.R., T.W.S., K.B.T., W.S.W., and A.W. performed research; J.P.K., D.J.K., B.J.C., J.E.A.T., J.L.B., I.R.D., J.M.E., D.F., R.B.F., A.C.G., I.I.-A., J.R.J., J.F.J.P., M.A.L., N.H.L., W.C.M., A.M.T.M., C.R.M., J.H.R., T.W.S., K.B.T., J.H.W., W.S.W., and A.W. analyzed data; and J.P.K., D.J.K., B.J.C., J.E.A.T., I.R.D., J.M.E., D.F., A.C.G., I.I.-A., J.F.J.P., N.H.L., W.C.M., A.M.T.M., C.R.M., J.H.R., K.B.T., W.S.W., and A.W. wrote the paper.

The authors declare no conflict of interest.

This article is a PNAS Direct Submission.

[1]To whom correspondence should be addressed. E-mail: kennett@geol.ucsb.edu.

[2]Retired.

This article contains supporting information online at www.pnas.org/lookup/suppl/doi:10.1073/pnas.1507146112/-/DCSupplemental.

and age reversals in stratigraphic sections (2, 7–9). For example, ^{14}C concentrations have varied unevenly over time for many reasons, including from carbon turnover in the deep oceans, fluctuations in Earth's magnetic field, the release of ^{14}C from biomass burning, influx of ^{14}C from long-period comets, and variations in cosmic radiation (solar and galactic and from supernovae; for details, see *SI Appendix, Dating Information*). In addition, there can be considerable uncertainty about the association of charcoal ages with paleontological and archaeological assemblages, caused by the vertical transport of charcoal in sedimentary sequences through many processes, including plant bioturbation (especially roots), animal bioturbation, and redeposition by wind, water, and ice. Furthermore, a measured ^{14}C date may be inaccurate for multiple reasons, including the old wood effect, or inbuilt age (7), as, for example, when burning a 200-y-old tree causes the fire's age to appear to be 200 y too old. Accuracy also may be affected by improper handling and pretreatment of samples before dating and by uncertainties in the current ^{14}C calibration curves. All of these problems currently make it impossible to date an end-glacial event with better than multidecadal to centennial accuracy, whether it is a Clovis campfire, mammoth kill site, or cosmic impact event. Regardless, dating uncertainties must be carefully addressed to obtain the best possible age estimates (see *SI Appendix, Dating Information* and Figs. S1 and S2).

Meltzer et al. (10) rejected 26 of 29 YDB sites, claiming that the ages of those sites do not fall within the previously published YDB age span of 12,950–12,650 Cal B.P. and thus could not have resulted from a single impact event (table 3 of ref. 10). Those authors criticized previous YDB age–depth models (11–13), but in doing so, they often improperly compared YDB dates by using median ages without considering inherent uncertainties, as discussed in site descriptions below and in *SI Appendix*.

In this contribution, we model the age of YDB deposits at 23 locations, chosen primarily because independent workers at all 23 sites had previously identified the stratum that corresponds in age to the Younger Dryas onset. In addition, at 17 of 23 sites, two or more independently published radiocarbon or optically stimulated luminescence (OSL) dates were already available, and the other 5 sites were previously dated by YDIH proponents (see *Methods* and *SI Appendix*, Tables S1 and S2 and Fig. S3, for details and map). Using Bayesian analyses, we address the following questions. (*i*) At each YDB site investigated, what is the best age estimate for the proxy-rich YDB layer? (*ii*) Do these modeled ages fall within the previously published YDB age range of 12,950–12,650 Cal B.P. (11–13)? (*iii*) What is the probability that the collective ages of the YDB layer resulted from a single isochronous event? (*iv*) If so, what is a revised probability age distribution for that event? (*v*) Is the modeled age of the YDB event consistent with the Younger Dryas onset, as determined by dates from the Greenland Ice Sheet, speleothems (cave deposits), lake cores, ocean cores, and tree rings? (*vi*) Have other researchers raised valid age-related issues (10, 14–17)?

To explore a climate connection, we modeled six records that report the age of earliest onset for the Younger Dryas, proposed to be coeval with the YDB cosmic impact event (1). We also compared all records to the age of the platinum peak reported in the Greenland Ice Sheet, interpreted by Petaev et al. (18) to mark a cataclysmic extraterrestrial impact event exactly at the earliest onset of the Younger Dryas climate episode. In addition to the 23 YDB sites, 9 sites display a variable assemblage of impact-related proxies, but they lack sufficient temporal and/or stratigraphic resolution for Bayesian statistical analysis and will be discussed only briefly.

The YDB chronology is the focus of this contribution, so, for further information about site descriptions, geological settings, archaeological and paleontological significances, and additional references, see individual sites discussed in *SI Appendix*. Previous papers have addressed the nature and origin of YDB impact-related proxies in detail, and, therefore, we consider these issues only briefly here. For more information, see the table that lists representative contributions by YDIH proponents, opponents, and independent researchers (*SI Appendix*, Table S2).

Results and Discussion

Calibrating Direct ^{14}C Dates. The process of radiocarbon calibration produces probability density functions, meaning that some unknown true age will fall within a specified age range at a certain percentage probability, e.g., 68%. In traditional statistics, those percentages are variously known as SDs or sigma (σ), but in Bayesian statistics, they are referred to as credible intervals, abbreviated here as CI. (19). Here, we use 68%, 95%, and 99% CI to represent degrees of uncertainty. A single calibrated calendar year is insufficient to represent the dating uncertainties involved, and thus, a probability, such as 68% or 95% CI, should always be assigned to each date (19, 20). Michczynski (21) observed that many researchers continue to present a single point date without reporting the uncertainties, due to convenience and simplicity, but doing so yields poor estimates of true ages. This is because there is only a very small statistical likelihood, typically <0.5%, that the median or mean date of a probability distribution represents the true calendar year for an event (Fig. 1).

Meltzer et al. (page 9 of ref. 10) ostensibly agreed with the criticism of point estimates and wrote, "Using just a single point estimate—whether a median, midpoint, or weighted mean—fails to account for uncertainties in the age estimate and thus leads to questionable regression results." Later, referring to their table 3 (10), they claimed, "9 of the 11 sites in this group have predicted ages for the supposed YDB that fall outside the YD onset time span." However, they contradicted their stated position by comparing YDB single dates without using the appropriate 68% or 95% probability. Furthermore, they did not use established principles of "chronological hygiene," meaning that, for example, they sometimes used an average age calculated from multiple charcoal dates from a single stratum. That practice is inappropriate when an old wood effect has been identified, in which case, short-lived samples (twigs, seeds, etc.) or the youngest dates from a single stratum should be given priority (*SI Appendix, Dating Information*) (2, 22).

For the nine YDB sites rejected by Meltzer et al. (10), one or more dates were acquired directly from the layer containing YDB impact proxies, in accordance with Telford et al. (8), who concluded that the age of any short-term event is best constrained by using dates from directly within or as close as possible to the event layer. To investigate, we used the IntCal13 curve within OxCal to calibrate the dates with uncertainties and

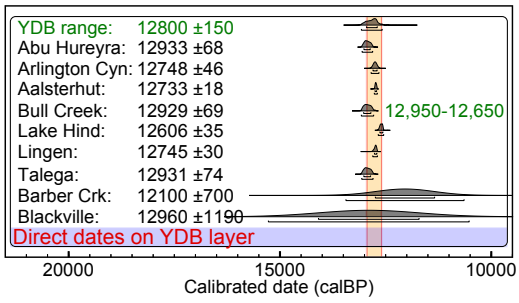

Fig. 1. Radiocarbon dates from directly within the YDB layer at nine localities. The published YDB age range is in green text; the vertical gold bar denotes the YDB age range of 12,950–12,650 Cal B.P. at 68%, which overlaps the age range distributions from all nine sites. Dates are from Kinzie et al. (9), except for Aalsterhut (15), Barber Creek (13), and Talega (13).

compared them with the previously published YDB age range. For these nine sites from four countries (United States, Canada, Germany, and Syria), geographically separated by ∼12,000 km, all nine YDB ages fall within the previously published YDB range of 12,950–12,650 Cal B.P. (Fig. 1). This finding contradicts Meltzer et al. (10) and agrees with previously published YDIH contributions (1, 9, 11–13).

Background for YDB Bayesian Analyses. Previously, proponents and opponents of the YDIH produced age–depth models using various types of regression algorithms. Even though widely used, regression models suffer from limitations, and, therefore, the use of Bayesian analyses to produce age models has become increasingly common (23–25). Such analyses can (*i*) calculate and compare millions of possible age models (iterations), unlike regression algorithms that calculate only one; (*ii*) integrate prior external information relevant to dating, e.g., the law of superposition (deepest is oldest); (*iii*) identify outlying dates that are too young or too old [e.g., the old wood effect (7)]; (*iv*) efficiently merge disparate data sets, e.g., from stratigraphy, archaeology, palynology, and climatology; (*v*) evaluate a cluster of dates for contemporaneity; (*vi*) overcome some of the inherent biases of various dating methods that tend to favor some calendar dates over others (26); and (*vii*) present a robust statistical model that explicitly represents all modeling assumptions and data input. Because of these advantages, Bayesian age–depth modeling is considered more robust and flexible than other types (23, 24), and, therefore, multiple disciplines now commonly use Bayesian analytical programs [e.g., BCal (27), BChron (28), OxCal (23, 24), and Bacon (25)]; see *SI Appendix*, *Dating Information* and *Methods*.

Bayesian Models for 23 Sites. For this paper, we used the IntCal13 calibration curve in the OxCal computer program for Bayesian statistical analysis (v4.2.4) (23, 24), which has three principal pertinent routines: ^{14}C calibration, calibrated age modeling, and contemporaneity testing. OxCal produces a modeled age distribution that is summarized in multiple ways, including as a mean age with uncertainties (±68% CI) and as a distribution of ages at 68%, 95%, and 99% CI. We used three different types of OxCal coding: (*i*) P_Sequence code, in which dates are associated with depths; (*ii*) Sequence code with Boundaries, for placing dates into groups with specified boundaries, between which the stratigraphic order is known, but exact depths are unknown or unclear; and (*iii*) Sequence coding with Phases, for placing dates into chronological groups, because the stratigraphic order is unknown or unclear.

All modeled ages were rounded to the nearest 5 y. For every site, we report the age ranges at 95% CI, along with the mean age and ±68% CI, because reporting both formats provides

YDB SITES (33)	Modeled ages	Uncertainty (68%)	Range, upper (95%)	Range, lower (95%)	# Total dates	# Rejected dates	# Accepted dates	Quality ranking	Date on proxies	Many dates	Climate indicators	Megafaunal remains	Paleolithic artifacts	Population hiatus	Few dates	Large uncertainties	Contradictory dates	Bioturbation	Redeposition
LOCATION	AGE		RANGE		DATES				STRENGTHS						DISADVANTAGES				
Abu Hureyra	12825	55	12935	12705	37	8	29	High	●	●	●	·	●	·	·	·	●	·	·
Arlington Cyn	12805	55	12925	12695	16	0	16	High	●	●	●	●	●	●	·	·	●	·	●
Aalsterhut	12780	35	12845	12725	14	0	14	High	●	●	●	·	·	●	·	·	·	·	·
Big Eddy	12770	85	12935	12580	30	2	28	High	·	●	●	·	●	·	·	·	·	·	●
Bull Creek	12840	75	12995	12710	12	0	12	High	●	●	●	●	●	·	·	·	·	·	·
Daisy Cave	12730	320	13320	12050	20	10	10	High	·	●	·	·	●	·	·	●	·	·	●
Lake Hind	12745	180	13190	12550	12	1	11	High	●	·	●	·	●	·	·	·	·	●	●
Lingen	12735	85	12910	12520	2	0	2	HIgh	●	·	●	·	●	●	●	·	·	·	·
Sheriden Cave	12840	120	13110	12625	30	1	29	High	·	●	●	●	●	●	·	·	·	·	●
Barber Creek	12865	535	13945	11865	14	1	13	Med	●	·	●	·	·	·	·	●	·	·	·
Blackwater	12775	365	13510	12090	29	1	28	Med	·	●	●	●	●	●	·	·	●	·	●
Indian Creek	12750	425	13495	11805	8	0	8	Med	·	·	·	·	●	·	·	·	·	·	·
Lindenmeier	12775	180	13195	12440	11	1	10	Med	·	·	●	·	●	·	·	·	·	·	·
Murray Spgs	12750	235	13195	12255	33	6	27	Med	·	●	●	●	●	●	·	·	●	·	·
Santa Maira	12785	295	13265	12070	11	0	11	Med	·	·	●	·	●	·	●	·	·	·	●
Talega	12860	150	13075	12545	12	0	12	Med	●	·	·	·	●	·	·	·	·	·	●
Topper	12785	185	13085	12365	11	0	11	Med	·	·	·	·	●	●	·	●	·	·	·
Blackville	12820	1080	15015	10705	5	2	3	Low	●	·	·	·	·	·	●	●	●	●	·
Lake Cuitzeo	12850	570	14265	12195	22	11	11	Low	·	·	●	●	·	·	●	●	●	·	●
Lommel	12735	790	14410	11325	17	1	16	Low	·	·	●	·	●	●	●	●	·	·	·
Melrose	12255	2405	17185	7710	3	1	2	Low	●	·	·	·	·	·	●	●	●	●	●
Mucunuque	12845	630	13550	11335	3	0	3	Low	·	·	●	·	·	·	●	·	·	·	·
Ommen	12750	560	13605	11425	2	0	2	Low	·	·	●	·	·	●	●	·	·	·	·
Chobot	·	·	·	·	3	·	·	x	·	·	●	·	●	·	●	●	●	●	·
Gainey	·	·	·	·	5	·	·	x	·	·	·	·	●	·	●	●	●	●	●
Kangerlussuaq	·	·	·	·	2	·	·	x	·	·	●	·	·	·	●	●	·	·	●
Kimbel Bay	·	·	·	·	7	·	·	x	·	·	·	·	·	·	●	●	·	●	●
Morley	·	·	·	·	·	·	·	x	·	·	●	·	·	·	●	·	·	●	·
Mt.Viso	·	·	·	·	·	·	·	x	·	·	●	·	·	·	●	·	·	·	·
Newtonville	·	·	·	·	2	·	·	x	·	·	●	·	·	·	●	·	·	●	·
Paw Paw Cove	·	·	·	·	1	·	·	x	·	·	●	·	·	·	●	·	·	·	●
Watcombe	·	·	·	·	2	·	·	x	·	·	●	·	·	·	●	·	·	·	·

Fig. 2. YDB site details. LOCATION column lists sites. AGE columns show Bayesian modeled ages at 68%; RANGE is at 95% CI. DATE columns list total dates used, dates accepted, and dates rejected by OxCal as outliers. QUALITY ranks as high, medium, low, and not modeled. STRENGTHS and DISADVANTAGES are listed by category.

greater clarity. After analyses of 354 dates at 23 YDB sites, the chronology for each site was ranked according to estimated quality, ranging from high to low, as discussed below (summarized in Fig. 2; for OxCal's coding, see *SI Appendix, Coding*).

High-Quality Chronologies. Bayesian statistical models for 9 of 23 sites are discussed in this section and in *SI Appendix*. These sites are considered high quality because they (*i*) mostly have ^{14}C dates from directly within the proxy-rich sample extracted from the YDB layer; (*ii*) have a high total number of dates per site (avg. 19 dates); (*iii*) have lower uncertainties than lesser quality dates (avg. 112 y); (*iv*) typically contain multiple temporally diagnostic indicators, including sedimentary and paleobiological records; and/or (*v*) usually contain temporally diagnostic cultural artifacts and megafaunal remains.

Abu Hureyra, Syria. This site was located on an archaeological mound, or "tell," ~14 km west of Al Thawra, Syria, and is now inundated by Lake Assad (29). The 5-cm-thick YDB sample was at a depth of 402.5–407.5 cm below surface (cmbs) and contained peaks in impact-related spherules, carbon spherules, nanodiamonds, and high-temperature melt glass and minerals (9, 12, 13).

For this site, the sequence of human cultural traditions is represented as Phases 1, 2, and 3 (the latter is the youngest), with the YDB layer occurring between Phases 1 and 2 (*SI Appendix*, Fig. S4). Based on changes in pollen and seeds, the YDB layer at Abu Hureyra is coeval with the Younger Dryas onset, which initiated significant cultural changes, including the adoption of early cultivation practices that later led to the emergence of agriculture in the Middle East (5, 29).

From a 7 × 7 m excavated pit, Moore et al. (29) acquired 37 ^{14}C dates, and OxCal generated a sequence-phase stratigraphic model using 29 of those dates and rejecting 8 dates as outliers (dates that appear either too young or too old for the statistical model). For details on rejection of outliers, see *SI Appendix, Prior Information in OxCal*. One ^{14}C date acquired from directly within the proxy-rich YDB sample has a modeled range of 12,935–12,705 Cal B.P. at 95% (12,825 ± 55 Cal B.P. at 68%). That date overlaps the previously published YDB age of 12,950–12650 Cal B.P. (*SI Appendix*, Fig. S4 and Table S3) (12, 13). For Abu Hureyra, Meltzer et al. (10) modeled a date of 13,044 Cal B.P. and claimed the YDB to be 144 y too old. However, they overlooked the presence of one age of 12,825 ± 55 Cal B.P. at 68% CI that is directly from the proxy-rich layer and falls within the YDB age range. Also, they presented a modeled YDB age as a point date without considering dating uncertainties.

Arlington Canyon, CA. This site is located on the northwest coast of Santa Rosa Island, one of California's Northern Channel Islands, ~52 km southwest of Santa Barbara (2, 13). Kennett et al. (2) sampled a 5.03-m-thick profile that includes the YDB layer, concluding that the sequence formed within a catchment basin that underwent rapid deposition at ~12,800 cal BP. The 111-cm-thick YDB stratigraphic section from 392 to 503 cmbs contains abundance peaks of impact-related spherules, nanodiamonds, carbon spherules, and aciniform carbon.

Kennett et al. (2) provided 16 dates, 12 of which are from directly within the proxy-rich YDB horizon. From these, OxCal modeled the dates in the proxy-rich YDB interval to obtain a YDB age of 12,805 ± 55 Cal B.P. at 68% (12,925–12,695 Cal B.P. at 95%) (Fig. 3 and *SI Appendix*, Table S4). Meltzer et al. (10) presented a median point date of 13,106 Cal B.P. and rejected the age of the Arlington Canyon YDB layer as being 308 y too old. However, their conclusion is incorrect, because they did not consider the uncertainties for their date and overlooked the substantial old wood effect from long-lived conifers that were widespread on the Channel Islands until ~12,800 y ago (2, 9).

Aalsterhut, Netherlands. Extending across northwestern Europe, the Usselo horizon is a buried eolian soil with high concentrations of charcoal at its upper boundary (15). The Usselo layer is buried by

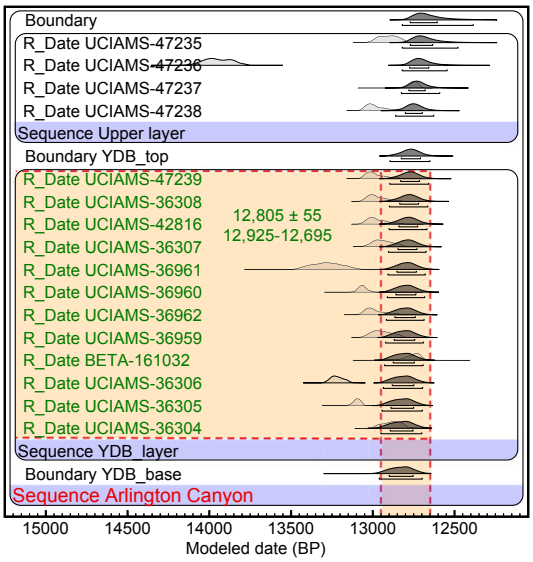

Fig. 3. Age sequence model for Arlington Canyon, CA. For this and chronological figures below, the vertical dashed lines represent the previously published YDB range of 12,950–12,650 Cal B.P. (9, 13). Horizontal red dashed lines represent the bounds of the proxy-rich sample. Laboratory numbers of dates are along the left side, with dates falling within the YDB interval shown in green text. R_Date represents ^{14}C dates, and C_Date, when present, represents OSL, varve, and ice layer calendar dates. OxCal's individual unmodeled probability distribution curves are shown in light gray, and modeled probability distributions are shown in dark gray. Boxed areas represent separate chronostratigraphic Phases or Sequences, and the probability distributions between phases represent the likely ages of transition. Phases mainly were identified by earlier site investigators in stratigraphic order, and dates within each Phase typically are in chronological order.

an overlying regional horizon, the Coversands, and the boundary between these lithologic units marks the onset or early years of the Younger Dryas episode (15). At the Aalsterhut site, van Hoesel et al. (15) reported nanodiamonds embedded in glass-like carbon from the top of the Usselo layer at a depth of 8.25–10 cm below the top of their sampled interval (they did not report the measured depth below surface).

Combining 14 ^{14}C dates, van Hoesel et al. (15) used OxCal to calculate an average median age for the entire 10-cm-thick section of 12,733 ± 18 Cal B.P. (recalibrated with IntCal13). However, 11 of the 14 dates are from the upper 8.25 cm, which contain no reported nanodiamonds. Because it is inappropriate to mix dates from nonproxy layers with those from the proxy-rich layer when dating a potential YDB layer, the average date reported by van Hoesel et al. (15) is incorrect, so we developed a new age model for the site using the same dates. OxCal used the three dates on the nanodiamond-rich interval from 8.25 cm to 10 cm to model an age range of 12,845–12,725 Cal B.P. at 95% (12,780 ± 35 Cal B.P. at 68%) (*SI Appendix*, Fig. S5 and Table S5).

van Hoesel et al. (15) compared their Aalsterhut age with that from Arlington Canyon and concluded that their nanodiamond-rich layer was not the YDB but instead postdated it by 200 y. However, that conclusion is contradicted by their own observation that the age of the Aalsterhut nanodiamond layer overlaps the age of the YDB layer at Murray Springs. Also, they did not consider the old wood effect, which makes their average age for Arlington Canyon too old (see *Arlington Canyon, CA*). Finally, they compared three YDB sites, but those had been calibrated with different ^{14}C calibration curves and had not been recalibrated, as is standard practice. To investigate the purported age difference, we obtained a Bayesian age range for Aalsterhut of 12,813–12,724 Cal B.P. at 95% CI that falls completely within

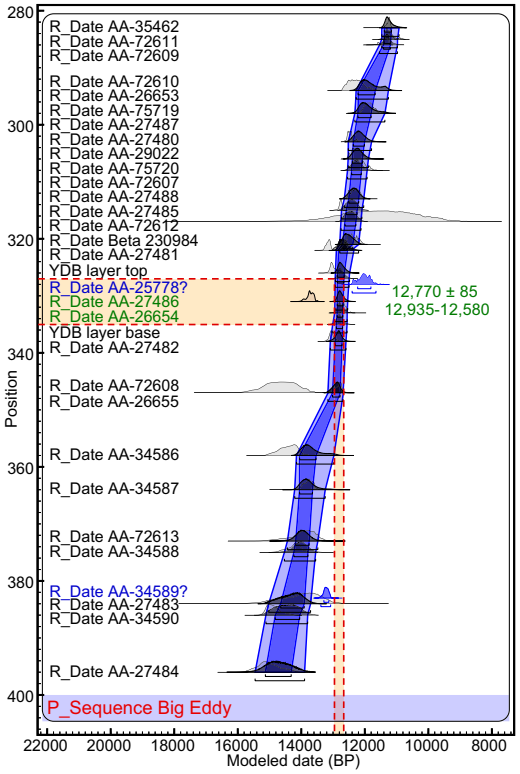

Fig. 4. Age–depth model for Big Eddy. The lighter blue continuous curve represents 95% probability, and the darker blue represents 68%. OxCal rejected the dates in blue text as outliers, meaning that they were statistically too old or young for the model.

the range for Arlington Canyon at 12,925–12,695 Cal B.P. at 95% CI. Thus, there is no 200-y age difference.

Big Eddy, MO. This site is located ∼4.5 km north of Stockton in the lower Sac River valley (13). The 8-cm-thick YDB sample contains a peak in YDB impact-related spherules at a depth of 327–335 cmbs. This site contains well-stratified, culturally rich deposits that include Clovis-age ^{14}C dates on a hearth feature and associated stone tools (13). To develop an age–depth model, we used 28 ^{14}C dates (10, 13) (Fig. 4 and *SI Appendix*, Table S6) and rejected 2 ^{14}C dates, consistent with the previous observation of redeposited charcoal (13). The age range for the YDB interval is 12,935–12,580 Cal B.P. at 95% (12,770 ± 85 Cal B.P. at 68%), matching the previously published YDB age.

Bull Creek, OK. This site lies along Bull Creek, an intermittent stream located in the panhandle of Oklahoma, where the 9-cm-thick YDB sample (298–307 cmbs) contained peaks in impact-related spherules, aciniform carbon, and nanodiamonds, which have been independently confirmed (9, 30). Of 12 available ^{14}C dates, 1 is reported at a depth of 307 cm from within the interval that included the nanodiamond-rich YDB sample (298–307 cmbs). The OxCal program generated a modeled YDB age of 12,995–12,710 Cal B.P. at 95% (12,840 ± 75 Cal B.P. at 68%), falling within the published YDB age range (*SI Appendix*, Fig. S6 and Table S7).

Daisy Cave, CA. Located ∼15 km west of Arlington Canyon, this cave–rockshelter complex is on the northeast coast of San Miguel Island, off the Southern California coast (9, 31). The YDB layer is at a depth of 79–81 cmbs and contains carbon spherules, glass-like carbon, and nanodiamonds. That layer's stratigraphic position is consistent with the palynological record, showing the transition from pine-dominated to oak-dominated forests in the area beginning at the Younger Dryas onset (31).

More than 20 AMS ^{14}C dates (10 on charcoal and 10 on shells) were acquired from a sample pit less than 1 m away from the stratigraphically correlated YDB profile. Only the 10 high-quality charcoal dates on short-lived samples (charred twigs) from this finely stratified sequence were used to generate a stratigraphic model for the YDB at the top of a darker layer, providing an age range of 12,730 ± 320 Cal B.P. at 68% (range of 13,220–12,050 Cal B.P. at 95%) (Fig. 5 and *SI Appendix*, Table S8).

Murray Springs, AZ. This well-known Clovis site is located 10 km east of Sierra Vista in a dry stream channel in the San Pedro Valley (13, 32, 33). The YDB layer is immediately beneath a black mat layer (33) at a depth of 246–247 cmbs and contains peaks in impact-related spherules, carbon spherules, aciniform carbon, nanodiamonds, melt glass, iridium, and nickel (1, 9, 13, 34).

We used 27 of 33 ^{14}C dates, acquired <40 m away from the sampling site, to produce a modeled age for the YDB of 12,750 ± 235 Cal B.P. at 68% (13,195–12,255 Cal B.P. at 95%). Previously, Haynes (33) reported an average calibrated age of 12,771 ± 47 Cal B.P. (recalibrated with IntCal13) based on eight dates associated with Clovis campfires from Unit F1, which is stratigraphically equivalent to the YDB layer. Likewise, Waters and Stafford (35) reported an average calibrated age of 12,761 ± 42 Cal B.P. (recalibrated with IntCal13) for the Clovis occupation layer. All these modeled ages closely correspond to each other and to the published YDB age (*SI Appendix*, Fig. S7 and Table S9).

Sheriden Cave, OH. This deeply stratified karst cavern is 4 km northwest of Carey, OH (13), where the YDB is a 1.5-cm-thick, charcoal-rich layer at a depth of 44.5–46.0 cmbs containing peaks in impact-related spherules, carbon spherules, and nanodiamonds. The YDB is closely associated with bones of the youngest known specimens of two extinct megafaunal species, the giant beaver (*Castoroides ohioensis*) with an age of 12,745 ± 45 Cal B.P. and the flat-headed peccary (*Platygonus compressus*) with a calibrated age of 12,920 ± 80 Cal B.P. The YDB layer is also closely associated with a Clovis flaked-stone projectile point and two Clovis bone projectile points that date to 12,765 ± 30 Cal B.P. Based on 29 of 30 AMS ^{14}C dates from across the 18-m-wide cave complex, the modeled age for this site is 12,840 ± 120 Cal B.P. at 68% (13,110–12,625 Cal B.P. at 95%) (Fig. 6 and *SI Appendix*, Fig. S8 and Table S10).

Medium-Quality Chronologies. Bayesian age–depth models for 8 of 23 sites are discussed in this section (see also *SI Appendix*). The chronologies for these sites are considered medium quality because the sites have (*i*) lower stratigraphic resolution, (*ii*) fewer

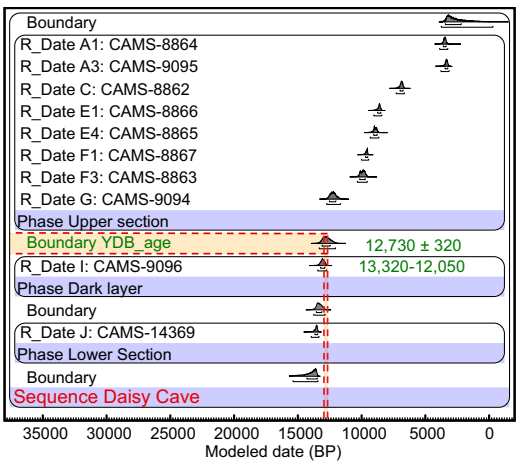

Fig. 5. Age sequence model for Daisy Cave, CA.

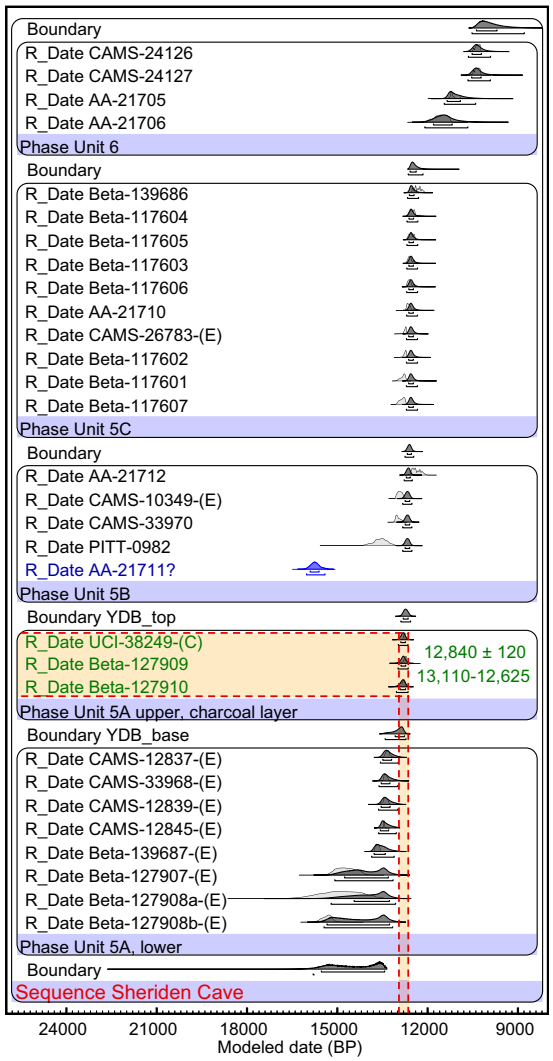

Fig. 6. Age sequence model for Sheriden Cave, OH.

dates per site (avg. 17 dates), (*iii*) larger uncertainties (avg. 295 y), and/or (*iv*) fewer temporally diagnostic indicators compared with the high-quality chronologies.

Barber Creek, NC. This next site is located ∼5.7 km east of Greenville, along a paleobraidplain near the confluence of the Tar River and Barber Creek (13). The YDB layer contained a peak in impact-related spherules at a depth of 97.5–100 cmbs, immediately above an abrupt stratigraphic change from alluvial to eolian deposition that marks the Younger Dryas onset. The stratigraphic position of Archaic and Woodland cultural artifacts is consistent with the age of the YDB layer.

Wittke et al. (13) reported an OSL date of 12,100 ± 700 Cal B.P. from directly within the YDB layer, but Meltzer et al. (10) rejected Barber Creek as a YDB site, because its median age is 700 y younger than the YDB. This conclusion is unfounded, because the probability distribution of that date (12,800–11,400 Cal B.P.) overlaps the published YDB range of 12,950–12,650 Cal B.P. (Fig. 7). We used 13 of 14 AMS ^{14}C and OSL dates from two excavation pits ∼10 m apart to produce an age model (*SI Appendix*, Table S11). The modeled age of the proxy-rich YDB layer is 12,865 ± 535 Cal B.P. at 68% (13,945–11,865 Cal B.P. at 95%), a span that falls within the previously published YDB range and has greater statistical certainty than the original OSL date as the result of Bayesian modeling.

Blackwater Draw, NM. Clovis projectile points were first discovered at this site, ∼18 km southeast of the city of Clovis. Sixteen sediment samples collected inside the South Bank Interpretive Center included a 1-cm-thick YDB sample at a depth of 250 cmbs (1237.55 m elevation). The YDB contained peak abundances in impact-related spherules, glass-like carbon, polycyclic aromatic hydrocarbons (PAHs), iridium, and nickel (1, 13, 36, 37). The YDB layer is located between Level C, the Clovis occupation surface, and Level D1, a diatomite layer that correlates with the black mat at >50 other sites across North America (33).

Based on stratigraphic relationships between 28 of 29 ^{14}C dates, we generated a Bayesian age model, in which the transition at the top of the YDB layer dates to 12,775 ± 365 Cal B.P. at 68% (13,510–12,090 Cal B.P. at 95%) (*SI Appendix*, Fig. S9 and Table S12). A YDB age is supported by abundant Clovis artifacts and mammoth bones in the layer immediately below the diatomite and by Folsom artifacts ∼20 cm above the diatomite. YDB impact-related spherules also were distributed across the original spoil from a hand-dug Clovis-age well (38) ∼50 m from the South Bank site, supporting the modeled age of the YDB layer.

Indian Creek, MT. Located ∼10 km west of Townsend, Indian Creek is a well-documented archaeological site, exhibiting a black mat layer containing Folsom cultural artifacts (33). A peak in nanodiamond-rich carbon spherules was found at a depth of 790–820 cmbs in the Clovis horizon immediately below the Folsom artifacts (9). Based on eight ^{14}C dates for the sequence, the age–depth model dates the top of the YDB layer to 12,750 ± 425 Cal B.P. at 68% (13,495–11,805 Cal B.P. at 95%), falling within the published YDB age span (*SI Appendix*, Fig. S10 and Table S13).

Lake Hind, Manitoba, Canada. Located in a cutbank along the Souris River in southwestern Manitoba, this site was once part of Glacial Lake Hind, an end-Pleistocene proglacial lake. At or near the Younger Dryas onset, ice dams on the lake failed in a regional pattern of meltwater flooding, transforming the lake from deep to shallow water (ref. 1 and references therein). The top of the YDB layer at a depth of 1,096–1,098 cmbs (avg., 1,097 cm) contains peaks in nanodiamonds, carbon spherules, nickel, and iridium. Eleven AMS ^{14}C dates were accepted and one was rejected in computing an age model that includes one date from directly within the proxy-rich YDB sample (*SI Appendix*, Fig. S11 and Table S14). The modeled age of the YDB layer is 12,745 ± 180 Cal B.P. at 68% (13,190–12,550 Cal B.P. at 95%), falling within the published YDB age range.

Lindenmeier, CO. Located in Larimer County, Colorado, ∼45 km north of Fort Collins (9), this site contains multiple Folsom-age

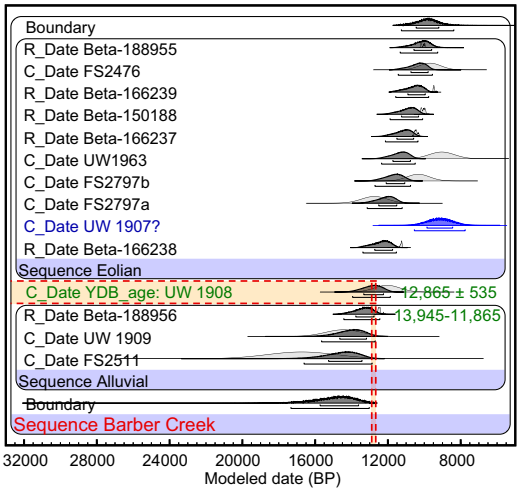

Fig. 7. Age sequence model for Barber Creek, NC.

encampments, associated with a black mat layer just above a peak in nanodiamonds found at a depth of 100–102 cm. The stratigraphic age model is based on 10 of 11 ^{14}C dates, producing a YDB age of 12,775 ± 180 Cal B.P. at 68% (13,195–12,440 Cal B.P. at 95%), which overlaps the published YDB range (*SI Appendix*, Fig. S12 and Table S15).

Lingen, Germany. Located along the Ems River in Germany, this site is approximately 1 km downstream from the bridge to Lingen (1, 13). As is typical of northwestern Europe and Aalsterhut, the Usselo layer at this site is enriched at the top in charcoal, signifying widespread biomass burning at the Younger Dryas onset. The YDB layer at a depth of 42–45 cmbs contained peaks in impact-related spherules and carbon spherules. One new ^{14}C date on charcoal from directly within the YDB layer calibrates to 12,735 ± 85 Cal B.P. at 68% (12,910–12,520 Cal B.P. at 95%), overlapping the YDB age range (*SI Appendix*, Fig. S13 and Table S16).

Lommel, Belgium. This site is 3 km west of the Lommel town center and exhibits a lithologic succession that includes the Usselo horizon, as discussed above for Aalsterhut and Lingen (1, 13). The charcoal-rich YDB layer at a depth of 47–50 cmbs contains peaks in impact-related spherules, carbon spherules, nanodiamonds, nickel, osmium, and iridium. Using 16 of 17 dates (16 OSL and 1 AMS ^{14}C), OxCal calculated a YDB age of 12,735 ± 790 Cal B.P. at 68% (14,410–11,325 Cal B.P. at 95%), within the published YDB age range (*SI Appendix*, Fig. S14 and Table S17).

Santa Maira, Spain. This limestone cave complex is ∼22 km from the Mediterranean Sea in the Alicante Province of eastern Spain (9). The YDB layer exhibits peaks in carbon spherules and nanodiamonds at a depth of 4–10 cmbs. Identification of the YDB layer is supported by the presence of temporally diagnostic changes in plant remains and cultural artifacts at the Younger Dryas onset (ref. 9 and references therein). Using 11 ^{14}C dates, OxCal generated an age sequence with a YDB age of 12,785 ± 295 Cal B.P. at 68% (13,265–12,070 Cal B.P. at 95%), which overlaps the YDB age range (*SI Appendix*, Fig. S15 and Table S18).

Talega, CA. Located ∼5 km northeast of San Clemente in the Santa Ana Mountains of Southern California, this site was sampled for an archaeological study using a platform-mounted auger to collect samples from deep boreholes (13). The proxy-rich YDB sample came from within a 30-cm interval (1,485–1,515 cmbs) that contained abundance peaks in impact-related spherules and carbon spherules. For Talega, Meltzer et al. (10) modeled an age of 13,030 ± 150 Cal B.P. (range: 13,180–12,880 Cal B.P.) and claimed that the date "does not fall within the temporal target of 12,800 ± 150 cal BP [range: 12,950 to 12,650]," even though it clearly does overlap. Using 12 spatially separated dates from the site, OxCal generated an age-sequence model with a YDB age of 12,860 ± 150 Cal B.P. at 68% (13,075–12,545 Cal B.P. at 95%), consistent with the published YDB age range (13) (*SI Appendix*, Fig. S16 and Table S19).

Topper, SC. This well-known Clovis-age quarry lies 17 km west of Allendale near the Savannah River (13). The YDB layer is a 5-cm-thick interval at a depth of 57.5–62.5 cmbs, exhibiting peaks in impact-related spherules, carbon spherules, nanodiamonds, nickel, chromium, and iridium intermixed with temporally diagnostic Clovis artifacts. LeCompte et al. (37) showed that YDB impact-related spherules were abundant in the sediment directly above and in contact with the chert artifacts but were absent directly beneath these artifacts. The sequence indicates that quarry use was interrupted for ∼600 y, beginning near the time the impact proxies were deposited, consistent with a major population decline/reorganization at the site (3). One AMS ^{14}C date from the layer containing abundant Clovis artifacts was used with 10 spatially separated OSL dates to determine a modeled age of 12,785 ± 185 Cal B.P. at 68% (13,085–12,365 Cal B.P. at 95%), which fall within the published YDB range (Fig. 8 and *SI Appendix*, Table S20).

Lower-Quality Chronologies. Bayesian age models for the remaining 6 of 23 sites are discussed in this section and are illustrated in *SI Appendix*. The sites are considered of lower quality because they (*i*) often include OSL dates, (*ii*) have larger uncertainties (avg. 1006 y), (*iii*) have fewer dates per site (avg. 9 dates), (*iv*) display more bioturbation and redeposition, and/or (*v*) contain fewer temporally diagnostic indicators.

Blackville, SC. This site is ∼3.2 km northwest of the town of Blackville (12, 13). The YDB layer occurs at a depth of 174–190 cmbs and exhibits peak abundances in impact-related spherules, high-temperature melt glass, carbon spherules, aciniform carbon, nanodiamonds, and iridium. Wittke et al. (13) reported an OSL date of 12,960 ± 1190 Cal B.P. from directly within the proxy-rich YDB layer. This age range (14,150–11,770 Cal B.P.) fully overlaps the published YDB age range, but Meltzer et al. (10) overlooked that range of uncertainties and claimed that Blackville is too old to be a YDB site. In OxCal, we used two of three OSL dates and one of two AMS ^{14}C dates to develop an age sequence with a modeled YDB age of 12,820 ± 1080 Cal B.P. at 68% (15,015–10,705 Cal B.P. at 95%) (*SI Appendix*, Fig. S17 and Table S21).

Lake Cuitzeo, Mexico. Israde-Alcántara et al. (11) analyzed samples in a 27-m-long core from the second largest lake in Mexico, covering 380 km^2 ∼26 km north of Morelia in the state of Michoacán. They found peaks in impact-related spherules, carbon spherules, and nanodiamonds at a depth of 277.5–282.5 cmbs. Kinzie et al. (9) acquired a new AMS ^{14}C date from a nearby shoreline sequence with a black mat layer and several tephra layers that were stratigraphically correlated with the lake core. OxCal used 11 of 22 ^{14}C dates to model a YDB age of 12,850 ± 570 Cal B.P. at 68% (14,265–12,195 Cal B.P. at 95%) (*SI Appendix*, Fig. S18 and Table S22). This site has a lower rank because of nine anomalously old outlier dates near the YDB layer that form two unusual, coherently linear age clusters of unknown origin.

Geochemical and paleolimnological evidence shows a significant climatic transition from warm temperatures, corresponding to the Allerød warm period, to cool temperatures, corresponding to the Younger Dryas (11). At Lake Cuitzeo, the transition occurred between two ^{14}C dates of 9,911 Cal B.P. and 18,755 Cal B.P., consistent with the age–depth model of Israde-Alcántara et al. (11). This warm-to-cool transition is identified as the onset of the Younger Dryas climatic episode, corresponding to evidence at other regional sites (11). We also investigated two alternate age–depth models, one of which excluded the shoreline date from Kinzie et al. (9) and produced a modeled YDB age of

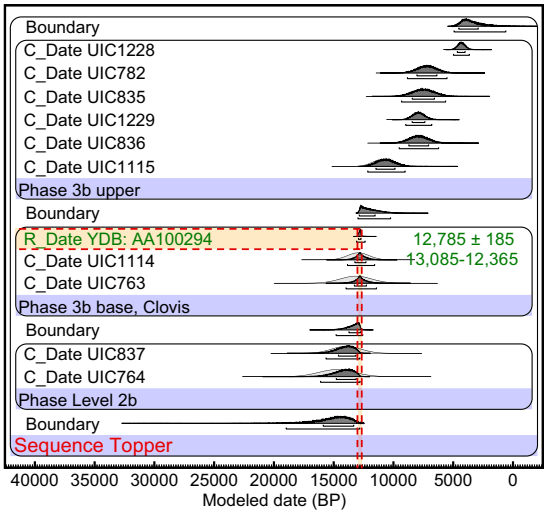

Fig. 8. Age sequence model for Topper, SC.

~15,300 Cal B.P. The other model that included the nine outliers produced a modeled YDB age of ~27,100 Cal B.P. However, both of these alternate YDB ages are inconsistent with the local and regional paleoclimatic record, and, hence, even though the lake is poorly dated, it is likely that the proxy-rich layer at Lake Cuitzeo is the same age as the YDB layer at well-dated sites.

Melrose, PA. This site is approximately 1 km southwest of Melrose in northeastern Pennsylvania (12, 13). The YDB layer spans an interval from 15 cmbs to 28 cmbs and contains a remarkable array of high-temperature impact proxies, including peaks in impact-related spherules, carbon spherules, aciniform carbon, nanodiamonds, high-temperature melt glass, nickel, and osmium (9, 12, 13, 39). The YDB age sequence model was based on one new AMS ^{14}C date and an OSL date of 11,701 ± 1846 Cal B.P. (equivalent to 11,640 y before 1950), taken from directly within the proxy-rich YDB sample. The modeled YDB age is 12,255 ± 2,405 Cal B.P. at 68% (17,185–7,710 Cal B.P. at 95%) (*SI Appendix*, Fig. S19 and Table S23).

Mucuñuque (MUM7b), Venezuela. This site is at an elevation of ~4,000 m in the Merida Province on the northwestern slope of the Cordillera Sierra de Santo Domingo in the Venezuelan Andes (40) and is farther south than any other well-studied YDB site. Recessional moraines and outwash fans representing the advance of area glaciers are undated at the site but are dated to the Younger Dryas nearby. The YDB layer lies at a depth of 210–213 cmbs beneath one of the Younger Dryas outwash fans and contains peaks in impact-related spherules, carbon spherules, quartz with planar features, and high-temperature melt glass. Using three dates directly from the site, OxCal generated an age sequence model with a YDB age of 12,845 ± 630 Cal B.P. at 68% (13,550–11,335 Cal B.P. at 95%), within the published YDB range (*SI Appendix*, Fig. S20 and Table S24).

Ommen, Netherlands. Located 3 km west of Ommen in the province of Overijssel, this site displays the Usselo Horizon, accepted to mark the Younger Dryas onset, as at Aalsterhut, Lingen, and Lommel (1, 13). The charcoal-rich YDB layer occurs at the top of the Usselo horizon at a depth of 115–120 cmbs and contains peaks in impact-related spherules, carbon spherules, and nanodiamonds. OxCal used two AMS ^{14}C dates to model the age of the YDB layer as 12,750 ± 560 Cal B.P. (13,605–11,425 Cal B.P. at 95% confidence interval), consistent with the previously published YDB range (*SI Appendix*, Fig. S21 and Table S25).

Other Sites. Nine other proxy-rich sites currently lack sufficient dating for robust Bayesian analysis. Even so, the stratigraphic context of a proxy-rich layer or samples at these sites supports a YDB age. These sites are Chobot, Alberta, Canada; Gainey, MI; Kangerlussuaq, Greenland; Kimbel Bay, NC; Morley, Alberta, Canada; Mt. Viso, France/Italy; Newtonville, NJ; Paw Paw Cove, MD; and Watcombe Bottom, United Kingdom. For further discussion, see *SI Appendix, Unmodeled Sites*.

Modeled vs. Unmodeled Ages. By design, Bayesian models alter some dates to produce statistically stronger age models. Therefore, the question arises of whether such changes cause errors by shifting the unmodeled YDB dates too old or too young. To investigate this for each of the 23 YDB sites, we selected the date closest to the median age of the YDB layer (12,800 ± 150 Cal B.P.) and calibrated each date with IntCal13 without using any Bayesian modeling (*SI Appendix, Methods*, Fig. S22 and Table S26). Of the 23 dates, 22 (96%) fall within the YDB range at 99% CI, and 19 (83%) overlap from 12,840–12,805 Cal B.P., a 35-y interval. These results indicate that Bayesian modeled ages are not substantially different from unmodeled calibrated ages.

Onset of Younger Dryas Climatic Episode. The YDIH posits that the Younger Dryas climate episode was triggered by the cosmic impact, and, therefore, the two should be contemporaneous (1).

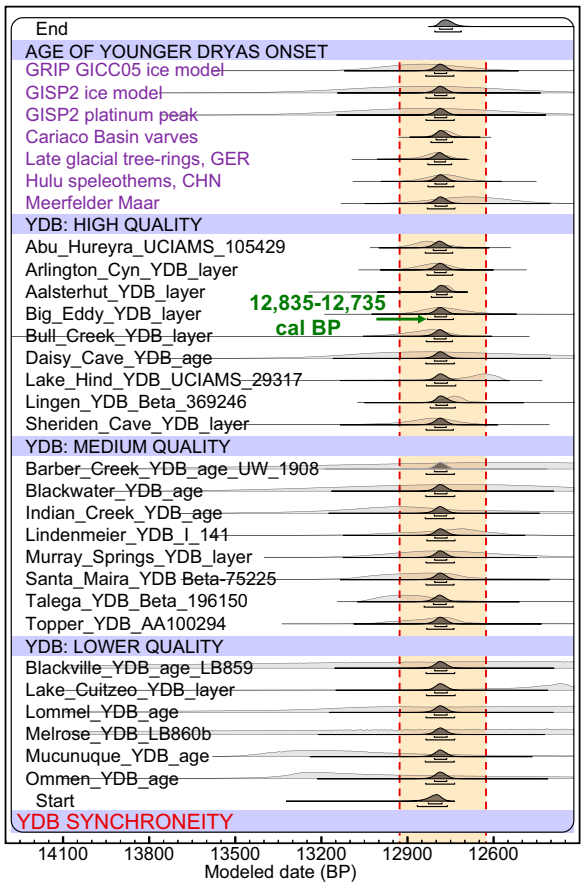

Fig. 9. Bayesian synchroneity tests of 30 records: 23 YDB sites with 1 GISP2 platinum peak and 6 independently dated climate records marking the Younger Dryas onset (purple text). For the 30 records, Sequence and Difference codes calculated the common age interval as ranging from 12,835 Cal B.P. to 12,735 Cal B.P. at 95% probability, as represented by the bottom black bar (at green arrow). Light gray probability distributions represent the individual modeled YDB ages for each record. Both light and dark gray distributions fall within the YDB age range of 12,950–12,650 Cal B.P. (yellow vertical bar).

Sometimes, multiple climate proxies are available for determining the onset of the Younger Dryas in a given record, and, if so, we used the earliest date in our Bayesian analyses, as others have done (41) (see *SI Appendix, Onset of Younger Dryas* and Table S27). The onset of the Younger Dryas has been independently dated in multiple records, representing a wide range of paleoenvironments in the Northern Hemisphere, including ice cores, tree rings, lake and marine cores, and speleothems, as follows [ice core dates are reported here as b2k (calendar years before base year AD 2000), consistent with glaciological convention; when compared with Cal B.P. dates (base year 1950), OxCal automatically adjusted b2k dates to Cal B.P. dates to be chronologically consistent]: (*i*) 12,896 ± 138 b2k (13,034–12,758 b2k), from several ice cores, Greenland Ice Core Project (GRIP), North Greenland Ice Core Project (NGRIP), and DYE-3 (42); (*ii*) 12,890 ± 260 b2k (13,150–12,630 b2k), from the Greenland Ice Sheet Program (GISP2) (43); (*iii*) 12,887 ± 260 b2k (13,147–12,627 b2k), for a peak in impact-related platinum, coeval with the onset of Younger Dryas cooling with the same uncertainty as the GISP2 core (18); (*iv*) 12,820 ± 30 Cal B.P. (12,850–12,790 Cal B.P.), from a count of annual varves in an ocean sediment core from the Cariaco Basin, Venezuela (44, 45); (*v*) 12,812 ± 49 Cal B.P. (12,861–12,763 Cal B.P.), from counting tree rings in the German pine record (46); (*vi*) 12,823 ± 60 Cal B.P. (12,883–12,763 Cal B.P.), based on oxygen isotope changes (δ^{18}O)

in speleothems from Hulu Cave, China (47); and (*vii*) 12,680 ± 127 varve years (before 1950 AD; 12,807–12,553 varve years; avg. error, 1%), a varve count for cores from Meerfelder Maar, Germany (48). The first six records above show striking similarities in both mean values and age ranges. Even though the mean ages of Meerfelder Maar and other varve records appear ∼200 y younger, all of the age estimates investigated overlap the previously published YDB age range of 12,950–12,650 Cal B.P. This leaves open the possibility that the Younger Dryas onset and the YDB impact event are synchronous.

YDB Datum Layer. In a number of sedimentary sections, individual types of YDB-like proxies have been observed intermittently in relatively low abundances outside of the YDB layer. However, only the YDB layer exhibits distinct abundance peaks in multiple impact-related proxies and, as such, forms a distinct, widely distributed event horizon or datum layer, similar, for example, to a geochemically distinctive volcanic tephra layer and the iridium-rich K–Pg impact layer. Existing stratigraphic information suggests that the YDB layer reflects the occurrence of a singular cosmic impact by a fragmented comet that resulted in widely distributed multiple impacts. The YDB datum concept as a singular event can be further tested through ultra-high-resolution chronostratigraphic investigations. This proposed datum layer should be synchronous over broad areas.

Synchroneity. We conducted a Bayesian test of synchroneity to explore whether the probability distributions overlap for all 23 YDB and 7 Younger Dryas onset dates and, therefore, the 30 sites could be contemporaneous. In accordance with the protocol for testing synchroneity, as described in Parnell et al. (49) and Bronk Ramsey (23), we used OxCal's Sequence and Difference codes to determine the duration of the most likely common age interval for the 30 records (Fig. 9). In this test, if the computed interval at 95% CI allows for a full overlap, i.e., includes zero years, then synchroneity is possible and is not rejected. On the other hand, if the estimated interval at 95% CI includes only nonzero values, then it is probable that the dated events occurred over a span of years, and synchroneity can be rejected. For the 30 sites, OxCal computed a minimum interval of zero years at 68% CI (range: 0–60 y). At 95% CI, the difference among the 30 sites ranges from 0 y to 130 y, and therefore, synchroneity is statistically possible and is not rejected.

Using the Difference code, we also calculated the modeled age span of the potential YDB overlap for the 30 sites. To do so, we used the Date code in OxCal with the Start and End Boundary ages to compute an age interval for the YDB event of 12,810–12,760 Cal B.P. (12,785 ± 25 Cal B.P.) at 68% CI and 12,835–12,735 Cal B.P. (12,785 ± 50 Cal. B.P.) at 95% CI. These ranges fall within the previously published YDB age range of 12,950–12,650 Cal B.P. For details, see *SI Appendix*, Table S28; for coding, see *SI Appendix, Coding*.

Additional support for synchroneity comes from the GISP2 ice core, in which a significant, well-defined, ∼18-y-long platinum peak was found in an ice interval spanning 279 y from 13,060–12,781 b2k (18). This single, short-duration platinum peak supports the occurrence of just one, rather than multiple events during that 279-y interval.

In summary, these statistical tests produced an overlapping unmodeled range of 12,840–12,805 Cal B.P. at 95% CI and an overlapping Bayesian-modeled range of 12,835–12,735 Cal B.P. Therefore, the 23 YDB age estimates appear isochronous within the limits of chronological resolution (∼100 y) and could have been deposited during a single event (*SI Appendix*, Tables S26 and S28). These findings refute the claim of Meltzer et al. (10) that YDB ages are asynchronous. Furthermore, the ages of the YDB at 23 sites are statistically contemporaneous with the independently determined onset of the Younger Dryas climate episode, suggesting a causal link between the two (*SI Appendix*, Tables S26 and S28).

Conclusions

Our results support six conclusions: (*i*) Bayesian analyses of 354 dates at 23 sites in 12 countries across four continents demonstrate that modeled YDB ages are consistent with the previously published range of 12,950–12,650 Cal B.P. (9, 11–13), contradicting claims that previous YDB age models are inaccurate (10, 14–16). (*ii*) Bayesian analyses indicate that YDB dates could be synchronous within the limits of uncertainties (∼100 y), contradicting claims that YDB dates are diachronous. (*iii*) Comparison with calibrated, unmodeled ages shows that Bayesian modeling does not significantly alter the calculated span of the YDB event. (*iv*) The ages of the 23 sites are coeval with the Younger Dryas onset in six records and with the age of deposition of extraterrestrial platinum in the GISP2 ice core at the Younger Dryas onset. This temporal relationship supports a causal connection between the impact event and the Younger Dryas. (*v*) These analyses produced a more refined modeled age for the YDB event of 12,835–12,735 Cal B.P. at 95% CI. Although Bayesian analysis alone cannot determine unequivocally that the YDB is synchronous at these 23 sites, a single event is the most plausible conclusion, given the widespread presence of peaks in impact-related spherules, melt glass, nanodiamonds, and other markers that all fall within a narrow temporal window of ∼100 y.

Methods

Sites for sampling were chosen because of accessibility and because Younger Dryas-aged strata already had been identified stratigraphically by independent workers (23 sites) and/or independently dated (18 of 23 sites). Radiocarbon dates (n = 354) were compiled from independent publications for 18 sites and from previous YDIH-group publications for the remaining 5 sites. We used all available dates, except in most cases where median dates were >15,000 Cal B.P. or <10,000 Cal B.P. in age; dates extending outside those limits were sometimes used when a site had only a few intermediate dates. For sites with widely scattered dates (Blackwater Draw and Murray Springs), we used only those dates within less than ∼60 m of the sampled section, on the assumption that those dates would provide the most accurate age model. Testing indicated that excluding such dates had no effect on the age–depth model between 13,100 Cal B.P. and 12,500 Cal B.P. We calibrated all dates using the IntCal13 dataset within OxCal v4.2.4 r:5 (23) and then calculated age models using Bayesian analyses in OxCal, based on the Markov chain Monte Carlo algorithm. We used standard codes and commands in OxCal, including P_Sequence, Sequence, and Phase. The Outlier code was also used because charcoal derives from vegetation that is, by necessity, older than the fire that carbonized it. OxCal's Difference code was used to explore potential synchroneity (for more details, see *SI Appendix, Methods*).

ACKNOWLEDGMENTS. For constructive comments that greatly improved this contribution, we are grateful to Andrew Parnell (University College Dublin, Ireland; developer of the BChron Bayesian program); Christopher Bronk Ramsey (University of Oxford, England; developer of the Bayesian program, OxCal); and Maarten Blaauw (Queen's University, Belfast, Northern Ireland; developer of the Bayesian program, Bacon). We also acknowledge the valuable time expended and efforts made by an anonymous reviewer.

1. Firestone RB, et al. (2007) Evidence for an extraterrestrial impact 12,900 years ago that contributed to the megafaunal extinctions and the Younger Dryas cooling. *Proc Natl Acad Sci USA* 104(41):16016–16021.
2. Kennett DJ, et al. (2008) Wildfire and abrupt ecosystem disruption on California's Northern Channel Islands at the Ållerød–Younger Dryas boundary (13.0–12.9 ka). *Quat Sci Rev* 27(27-28):2530–2545.
3. Anderson DG, Goodyear AC, Kennett J, West A (2011) Multiple lines of evidence for possible human population decline/settlement reorganization during the early Younger Dryas. *Quat Int* 242(2):570–583.
4. Jones TL, Kennett DJ (2012) A land impacted? The Younger Dryas Boundary event in California. *Contemporary Issues in California Archaeology*, eds Jones TL, Perry JE (Left Coast Press, Walnut Creek, CA), pp 37–48.

5. Moore AMT, Kennett DJ (2013) Cosmic impact, the Younger Dryas, Abu Hureyra, and the inception of agriculture in Western Asia. *Eurasian Prehist* 10(1-2):57–66.
6. Kennett DJ, Culleton BJ, Dexter J, Mensing SA, Thomas DH (2014) High-precision AMS ^{14}C chronology for Gatecliff Shelter, Nevada. *J Arch Sci* 52:621–632.
7. Schiffer MB (1986) Radiocarbon dating and the "old wood" problem: The case of the Hohokam chronology. *J Archaeol Sci* 13(1):13–30.
8. Telford RJ, Heegaard E, Birks HJB (2004) All age–depth models are wrong: But how badly? *Quat Sci Rev* 23(1-2):1–5.
9. Kinzie CR, et al. (2014) Nanodiamond-rich layer across three continents consistent with major cosmic impact at 12,800 cal BP. *J Geol* 122(5):475–506.
10. Meltzer DJ, Holliday VT, Cannon MD, Miller DS (2014) Chronological evidence fails to support claim of an isochronous widespread layer of cosmic impact indicators dated to 12,800 years ago. *Proc Natl Acad Sci USA* 111(21):E2162–E2171.
11. Israde-Alcántara I, et al. (2012) Evidence from central Mexico supporting the Younger Dryas extraterrestrial impact hypothesis. *Proc Natl Acad Sci USA* 109(13):E738–E747.
12. Bunch TE, et al. (2012) Very high-temperature impact melt products as evidence for cosmic airbursts and impacts 12,900 years ago. *Proc Natl Acad Sci USA* 109(28): E1903–E1912.
13. Wittke JH, et al. (2013) Evidence for deposition of 10 million tonnes of impact spherules across four continents 12,800 y ago. *Proc Natl Acad Sci USA* 110(23): E2088–E2097.
14. Boslough MB, et al. (2012) Arguments and evidence against a Younger Dryas impact event. *Climates, Landscapes, and Civilizations*, Geophysical Monograph Series, eds Giosan L, Fuller DQ, Nicoll K, Flad RK, Clift PD (Am Geophys Union, Washington, DC), Vol 198, pp 13–26.
15. van Hoesel A, et al. (2012) Nanodiamonds and wildfire evidence in the Usselo horizon postdate the Allerod–Younger Dryas boundary. *Proc Natl Acad Sci USA* 109(20): 7648–7653.
16. van Hoesel A, et al. (2014) The Younger Dryas impact hypothesis: A critical review. *Quat Sci Rev* 83(1):95–114.
17. Blaauw M, Holliday VT, Gill JL, Nicoll K (2012) Age models and the Younger Dryas impact hypothesis. *Proc Natl Acad Sci USA* 109(34):E2240, author reply E2245–E2247.
18. Petaev MI, Huang S, Jacobsen SB, Zindler A (2013) Large Pt anomaly in the Greenland ice core points to a cataclysm at the onset of Younger Dryas. *Proc Natl Acad Sci USA* 110(32):12917–12920.
19. Millard AR (2014) Conventions for reporting radiocarbon determinations. *Radiocarbon* 52(2):555–559.
20. Blaauw M (2010) Methods and code for 'classical' age-modelling of radiocarbon sequences. *Quat Geochronol* 5(5):512–518.
21. Michczynski A (2007) Is it possible to find a good point estimate of a calibrated radiocarbon date? *Radiocarbon* 49(2):393–401.
22. Erlandson JM, Braje TJ, Graham MH (2008) How Old is MVII? Seaweeds, shorelines, and the pre-Clovis chronology at Monte Verde, Chile. *J Island Coast Archaeol* 3:277–281.
23. Bronk Ramsey C (2009) Bayesian analysis of radiocarbon dates. *Radiocarbon* 51(1): 337–360.
24. Bronk Ramsey C, Lee S (2013) Recent and planned developments of the program OxCal. *Radiocarbon* 55(2-3):720–730.
25. Blaauw M, Christen JA (2011) Flexible paleoclimate age-depth models using an autoregressive gamma process. *Bayesian Anal* 6(3):457–474.
26. Bronk Ramsey C (1998) Probability and dating. *Radiocarbon* 40(1):461–474.
27. Buck CE, Christen JA, James GN (1999) BCal: An on-line Bayesian radiocarbon calibration tool. *Internet Archaeol* 7:dx.doi.org/10.11141/ia.7.1.
28. Haslett J, Parnell A (2008) A simple monotone process with application to radiocarbon-dated depth chronologies. *J R Stat Soc Ser C* 57(4):399–418.
29. Moore AMT, Hillman GC, Legge AJ (2000) *Village on the Euphrates* (Oxford Univ Press, New York).
30. Bement LC, et al. (2014) Quantifying the distribution of nanodiamonds in pre-Younger Dryas to recent age deposits along Bull Creek, Oklahoma panhandle, USA. *Proc Natl Acad Sci USA* 111(5):1726–1731.
31. Erlandson J, et al. (1996) An archaeological and paleontological chronology for Daisy Cave (CA-SMI-261), San Miguel Island, California. *Radiocarbon* 38(2):355–373.
32. Haynes CV, Jr (1998) Arizona's famous Clovis sites could be displayed for public. *Mammoth Trumpet* 13(2):2–6, 20.
33. Haynes CV, Jr (2008) Younger Dryas "black mats" and the Rancholabrean termination in North America. *Proc Natl Acad Sci USA* 105(18):6520–6525.
34. Fayek M, Anovitz LM, Allard LF, Hull S (2012) Framboidal iron oxide: Chondrite-like material from the black mat, Murray Springs, Arizona. *Earth Planet Sci Lett* 319: 251–258.
35. Waters MR, Stafford TW, Jr (2007) Redefining the age of Clovis: Implications for the peopling of the Americas. *Science* 315(5815):1122–1126.
36. Firestone RB (2009) The case for the Younger Dryas extraterrestrial impact event: Mammoth, megafauna, and Clovis extinction, 12,900 years ago. *J Cosmol* 2:256–285.
37. LeCompte MA, et al. (2012) Independent evaluation of conflicting microspherule results from different investigations of the Younger Dryas impact hypothesis. *Proc Natl Acad Sci USA* 109(44):E2960–E2969.
38. Haynes CV, Jr, et al. (1999) A Clovis well at the type site 11,500 B.C.: The oldest prehistoric well in America. *Geoarchaeol* 14(5):455–470.
39. Wu Y, Sharma M, LeCompte MA, Demitroff MN, Landis JD (2013) Origin and provenance of spherules and magnetic grains at the Younger Dryas boundary. *Proc Natl Acad Sci USA* 110(38):E3557–E3566.
40. Mahaney WC, et al. (2010) Evidence from the northwestern Venezuelan Andes for extraterrestrial impact: The black mat enigma. *Geomorphology* 116(1-2):48–57.
41. Steffensen JP, et al. (2008) High-resolution Greenland ice core data show abrupt climate change happens in few years. *Science* 321(5889):680–684.
42. Rasmussen SO, et al. (2006) A new Greenland ice core chronology for the last glacial termination. *J Geophys Res* 111(D6):D06102.
43. Meese DA, et al. (1997) The Greenland Ice Sheet Project 2 depth-age scale: Methods and results. *J Geophys Res* 102(C12):26411–26423.
44. Lea DW, Pak DK, Peterson LC, Hughen KA (2003) Synchroneity of tropical and high-latitude Atlantic temperatures over the last glacial termination. *Science* 301(5638): 1361–1364.
45. Haug GH, Hughen KA, Sigman DM, Peterson LC, Röhl U (2001) Southward migration of the intertropical convergence zone through the Holocene. *Science* 293(5533): 1304–1308.
46. Kromer B, et al. (2004) Late glacial ^{14}C ages from a floating, 1382-ring pine chronology. *Radiocarbon* 46(3):1203–1209.
47. Wang YJ, et al. (2001) A high-resolution absolute-dated late Pleistocene Monsoon record from Hulu Cave, China. *Science* 294(5550):2345–2348.
48. Brauer A, Endres C, Negendank JF (1999) Lateglacial calendar year chronology based on annually laminated sediments from Lake Meerfelder Maar, Germany. *Quat Int* 61(1):17–25.
49. Parnell AC, et al. (2008) A flexible approach to assessing synchroneity of past events using Bayesian reconstructions of sedimentation history. *Quat Sci Rev* 27(19-20): 1872–1885.